Open access • Journal Article • DOI:10.1109/TPWRS.2011.2180741

Investigation of Voltage Stability for Residential Customers Due to High Photovoltaic Penetrations — Source link

Ruifeng Yan, Tapan Kumar Saha

Institutions: University of Queensland

Published on: 31 Jan 2012 - IEEE Transactions on Power Systems (IEEE)

Topics: Grid-connected photovoltaic power system, Photovoltaic system, Low voltage, Voltage regulator and Maximum power point tracking

R. Yan and T. K. Saha (Corresponding Author), "Investigation of Voltage Stability for Residential Customers due to High Photovoltaic Penetrations", IEEE Transactions on Power Systems, Vol. 27, No. 2, pp. 651-662, May 2012. DOI: 10.1109/TPWRS.2011.2180741

Investigation of Voltage Stability for Residential Customers due to High Photovoltaic Penetrations

Ruifeng Yan, *Student Member, IEEE*, and Tapan Kumar Saha, *Senior Member, IEEE*

***Abstract*—Several studies on voltage stability analysis of electric systems with high photovoltaic (PV) penetration have been conducted at a power transmission level, but very few have focused on small area networks of low-voltage. As a distribution system has its special characteristics – high R/X ratio, long tap switching delay, small PV units and so on, PV integration impacts also need to be investigated thoroughly at a distribution level. In this paper, the IEEE 13 bus system has been modified and extended to explore network stability impacts of variable PV generation and the results show that a voltage stability issue with PV integration does exist in distribution networks. Simulation comparisons demonstrate that distribution networks are traditionally designed for heavily loaded situations exclusive of PVs, but they can still operate under low PV penetration levels without cloud induced voltage stability problems. It is also demonstrated that voltage instability can effectively be solved by PV inverter reactive power support if this scheme is allowed by the standards in the near future.**

***Index Terms*—Photovoltaic, voltage stability, distribution system, PV integration.**

I. Introduction

PHOTOVOLTAIC (PV) power is becoming less expensive every year, thus its growth is expected to be much greater in the near future. As PV penetration levels increase, its integration impact on electric networks draws researcher's concerns around the world. During the last decade a great amount of research has been carried out in this field.

The well known PV integration effect – voltage rise, was presented in the National Renewable Energy Laboratory (NREL) report [1] and several voltage control methods were considered in static analysis, such as inverter reactive power injection, on-load tap changer (OLTC) and switched capacitor. Another NREL report in 2008 provided dynamic analysis of large scale PV penetration at the transmission level [2]. It mainly focused on power network responses after contingencies – generation trip, load trip and fault. Whitaker summarized PV integration research since 1985 [3]. Cloud transient effects attracted much attention and its induced power swing and ramp following capability issues were recognized, but generally there were no serious voltage stability problems reported. Voltage fluctuation caused by cloud transients was described in a Sandia report and it was regarded to be smooth and slow [4]. It stated fluctuation might be a problem when PV penetration exceeds 20%. However, no detailed analyses were presented.

Many methods have been developed to tackle the variable characteristics of PV generation. Power curtailment was proposed in [5, 6] for understanding of overvoltage problems. This method requires estimating maximum PV power available under any weather conditions, but it is hard to acquire this information when sun radiation is changing fast. By using energy storage devices and appropriate control of charge/discharge, PV variations can be managed [7, 8].

PV inverter reactive power support is a well accepted method for voltage support [9-11], although it is against current standards [12, 13]. This method utilizes the ability of inverters to behave as small Flexible AC Transmission Systems (FACTS) devices for voltage regulation. However, in general it requires more expensive oversize inverters and this is not a common practice for small PV units in distribution systems. Recently researchers started to explore opportunities of applying active network management to voltage control, which is basically coordination and intelligent control built on the assumption of widespread communication infrastructure availability [14-16].

In the literature, PV cloud effects on voltage stability were investigated mainly in either a large scale transmission level or an individual unit control level with a simple network. Yun Tiam implemented a PV reactive power control method for voltage regulation to deal with voltage fluctuations during large irradiation changes, but it is still at a transmission level [17]. Low-voltage distribution networks have their special characteristics, for example unbalanced nature, line drop compensation (LDC) device, small size PVs, dynamic loads (small induction motors and thermostats), high R/X ratio [18] and so on. Steady and reliable performance in a large scale transmission system does not necessarily mean the same performance can be achieved in a geographically small distribution system as the local network can lose almost all PV power support in the area due to cloud coverage within a short period. Such a system is important and needs to be examined thoroughly, but currently few detailed analyses are available on this issue. This paper presents a potential voltage stability problem of high PV penetration in a geographically small network due to fast PV power swings. It is investigated under the current standards and industrial practices for small-scale grid-connected PV systems, in which PV reactive power generation for the voltage regulation purpose is forbidden and seldom implemented. A PV reactive power support scheme is developed to demonstrate its effectiveness if this strategy is permitted by the standards in the near future.

R. Yan (ruifeng@itee.uq.edu.au) and T. K. Saha (saha@itee.uq.edu.au) are with School of Information Technology & Electrical Engineering, University of Queensland, Australia.

In this paper, Section II presents details of the components in the network, including the IEEE 13 bus load modification, load models, tap changer settings and PV systems. This provides necessary information to further understand the development of voltage instability. In Section III, cloud effects on voltage stability of the system is investigated with different PV penetration levels using dynamic loads. To demonstrate the importance of implementing the detailed dynamic load models, Section IV compares the results from Section III with those applying the static loads. Potential Solutions to the voltage problem are presented in Section V, and battery storage and PV inverter reactive power support are analyzed in detail. Section VI summarizes simulation results, and Section VII discusses some important observations. Finally, conclusions are drawn in Section VIII.

II. Power System Used For Study

The IEEE 13 bus system is an unbalanced network containing many characteristics of a typical distribution network (Fig. 1).

(1) Three phase, two phase and single phase lines and cables with significant mutual coupling
(2) Delta and star connected loads and distributed loads in three types – constant power, constant current and constant impedance (ZIP types)
(3) A LDC voltage regulator
(4) Two three-phase transformers and a circuit breaker

The network was constructed in PSCAD/EMTDC environment [19] and was modified for the purpose of voltage stability analysis and PV power integration.

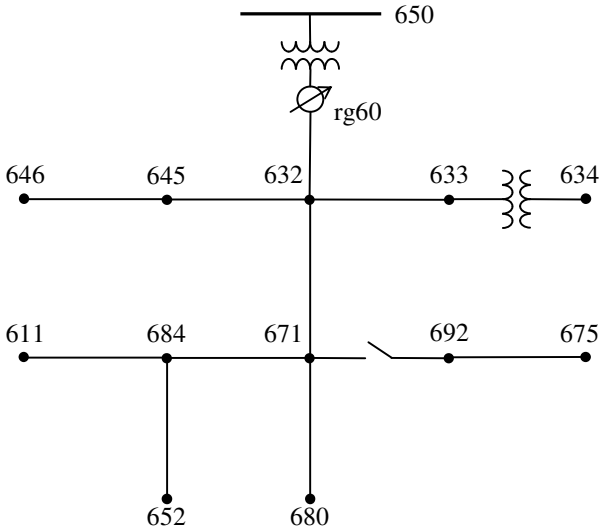

Fig. 1. IEEE 13 node test feeder [20]

A. Modified IEEE 13 Bus System

A typical weather condition assumed in this study is described as follows:

(1) Hot summer
(2) 35℃ ambient temperature
(3) $1000W/m^2$ sunlight irradiation
(4) Fast moving clouds in the sky

Therefore, under this weather condition a heavily loaded power system is expected. The loading status of the IEEE 13 node test feeder is modified as shown in Table I.

Except the delta-connected loads and Bus 634 loads, all other loads are connected to the network through single-phase transformers, which convert nominal 2.4018kV to 240V. Because these transformers have similar power and voltage ratings to the transformer between Bus 633 and Bus 634, the same per unit impedance rating is assumed for all added transformers.

TABLE I
Modification of the IEEE 13 Bus System Spot Loads

Node-Phase	Load Model	Original Load		Modified Load	
		kW	kVAr	kW	kVAr
634-B	Y-PQ	120	90	181	90
634-C	Y-PQ	120	90	168	90
645-B	Y-PQ	170	125	251	125
675-B	Y-PQ	68	60	120	60
675-C	Y-PQ	290	212	396	212
692-C	D-I	170	151	282	151

The loading information is summarized in Table II. The maximum capacity of this system is 5MVA, which means 1.67MVA for each phase. The loading levels of phase-B and phase-C have been increased after modification, but the nominal loading power is still within the limits of all phases and the overall system.

TABLE II
Summary of the IEEE 13 Bus System Loading Statues

Phases	Original Load		Modified Load		Capacitor Banks	Apparent (Modified Load)
	kW	kVAr	kW	kVAr	kVAr	kVA
PH-A	1175	616	1175	616	200	1246.47
PH-B	1039	665	1233	665	200	1317.77
PH-C	1252	821	1518	821	300	1604.92
Total	3466	2102	3926	2102	700	4168.82

B. Detailed Load Modeling

1) Load Combination

Dynamic load models are implemented in the simulation. Without any detailed information of load characteristics, typical data can be adopted for load modeling in residential areas, 25% resistive loads and 75% small motor loads [21]. Because of the introduction of low voltage transformers, the induction motors are designed to absorb slightly less reactive power than the nominal values to compensate for reactive power losses in the added transformers. The load combination is illustrated in Table III – around 25% resistive loads (resistor and thermostats) and 75% small motor loads. More details can be found in the Appendix. The total loads are within the transformer capacity limits and represent the power consumption at the time of simulation. The loading level should not be regarded as the maximum level with all appliances switched on. Because of the diversity of the load, not all electrical devices are operating at the same time.

TABLE III
THE IEEE 13 BUS SYSTEM LOAD COMBINATIONS

Load	kW or kVAr	S (kVA)	(P/Ptotal)%	(S/Stotal)%
Resistor & Thermostats	P=513.77	1027.54	26.2%	24.7%
	P=513.77			
Motor & Capacitor	P=2898.46	3201.97	73.8%	75.3%
	Q=1360.70			
Total	P=3926.00	4155.11	–	–

2) Induction Motor Load

It is crucial to include dynamic induction motor models for voltage stability analysis; however it is nearly impossible to consider every detail of contribution from different induction motors in a simulation. Therefore, a fifth-order aggregated induction motor model was constructed using residential room air conditioner parameters [22]. The induction motor was chosen to be fully loaded (1.0 pu loading torque) corresponding to hot weather conditions. The stalling voltage is around 0.87 to 0.88 pu, which is within the typical range [22, 23]. When one motor starts to stall, it will draw approximately three times normal current, which may cause adjacent motors to stall although their stalling voltages are lower [22]. Thus, it is adequate to use this room air conditioner to represent an aggregated induction motor load.

According to the load combination, small induction motors should consume all reactive power of the system loads, but the real/reactive power ratio of the aggregated induction motor under the nominal voltage (1.0 pu) is fixed (Fig. 2). Therefore, real power values of some spot loads have to be changed to accommodate the motor P/Q ratio, to achieve 25% resistive loads and to represent hot weather conditions – a heavily loaded network. The IEEE 13 bus load modifications (Table I) were calculated based on this principle.

A capacitor-start circuit (Fig. 3) is designed to start the single phase room air conditioner. The starting torque at the nominal voltage, which should generally be 2 to 3 times the rated torque [25], was selected to be about 2.45 (Fig. 4 (a)). Fig. 4 (b) shows torque curves at the voltage of 0.87 pu where the motor begins to stall. Both starting torque and operating torque decrease with the grid voltage.

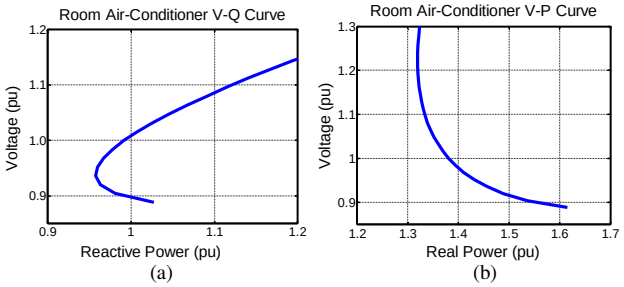

Fig. 2. Room air-conditioner V-Q and V-P curves

A centrifugal switch is modeled to disconnect the start winding of an induction motor. It will detach an auxiliary winding when a motor reaches 80% of synchronous speed and connect the winding when its speed is lower than 40%, which gives a cut-out/cut-in ratio of 2 [26].

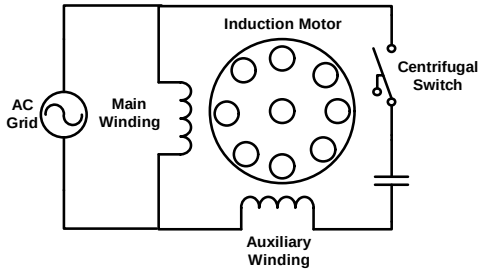

Fig. 3. Induction motor circuit [24]

Normally small induction motors on appliances are only equipped with thermal overload protection devices, which normally disengage stalling motors within 3 to 30 seconds [22]. The thermal protection implemented in the simulation calculates accumulated heat caused by over-current and the protection will disconnect the motor once heat reaches a preset value, which is equivalent to the heat generated by the maximum stalling current for 3 seconds.

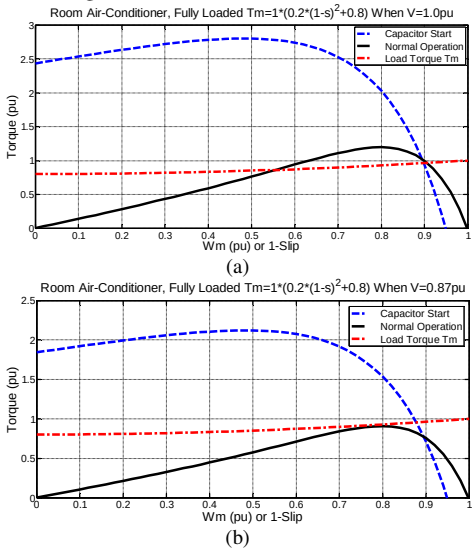

Fig. 4. Induction motor torque curves

3) Thermostatic Load

Thermostatic loads which account for half of resistive power are also simulated (Fig. 5). When grid voltage drops, more thermostatic loads will keep powered for a longer period, thus collectively they tend to recover power consumption during the drop. However, power recovery has to have a limit. When the voltage decreases to a certain low level, all thermostatic loads will be connected and thereafter thermostatic power can only decline with voltage and cannot be restored over time. In this study, the recovery time constant is 100s and the maximum thermostatic power under the nominal voltage is 1.5 times the rated load. The characteristics are shown in Fig. 6.

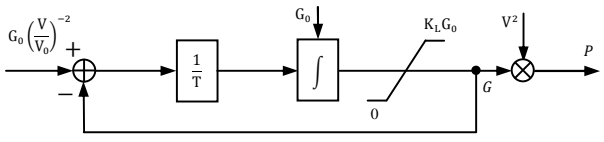

Fig. 5. Thermostatic load model [22]

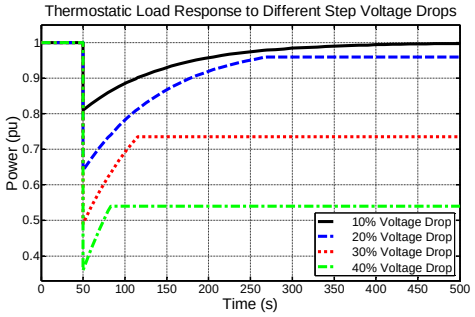

Fig. 6. Thermostatic load response

C. Voltage Regulator

The voltage regulator in the simulation adopts the typical parameters for distribution systems. It has 32 tap positions (± 16) with 0.00625 pu voltage per tap and $\pm 10\%$ voltage regulation range [27] and was confirmed by IEEE 13 bus power flow results [20].

In general, voltage regulators should have a hysteresis characteristic to reduce sensitivity and avoid unnecessary tap changes because excessive operation can shorten its life time. A $\pm 0.6V$ hysteresis band was selected in the simulation.

The tap changer is a mechanical device so it will take time to move from one position to the next. Commonly this time period is about 5 to 10 seconds [22]. In a large power system every voltage level has its own tap changer. In order to reduce the possibility of the tap changers hunting each other and establishing a better coordination, the common practice is to make the higher voltage level tap changers respond faster than those in lower voltage networks [28]. Usually, the first tap time delay for distribution tap changers is from 30 to 60 seconds [22].

D. Photovoltaic System

1) Photovoltaic Model

The single-phase PV system in the simulation is connected to the low voltage network (240V). To reduce computational complexity a current controlled source PV model is implemented (Fig. 7) and the dynamic behavior of this model is almost the same as the detailed model using power electronic components [29].

In the simplified model the switching frequency of the power electronic devices (e.g. DC-DC boost converter and PWM inverter) have been eliminated; therefore a lower sampling frequency can be applied to ensure an acceptable simulation speed. In Fig. 7 only the necessary control parts – maximum power point tracking and unity power factor control – are kept in the model, while high frequency switching elements are no longer a part of the model. The details can be found in [29].

According to the current standards – IEEE 1547 and IEEE 929, small PV units are not allowed to inject reactive power to power networks for voltage regulation purposes. Moreover, reactive power generation can put more stress on inverters and receive no financial benefit in return, so real power production is preferable and most PV systems are controlled close to unity power factor [12]. Therefore, all PV systems in the simulation only deliver real power to the network.

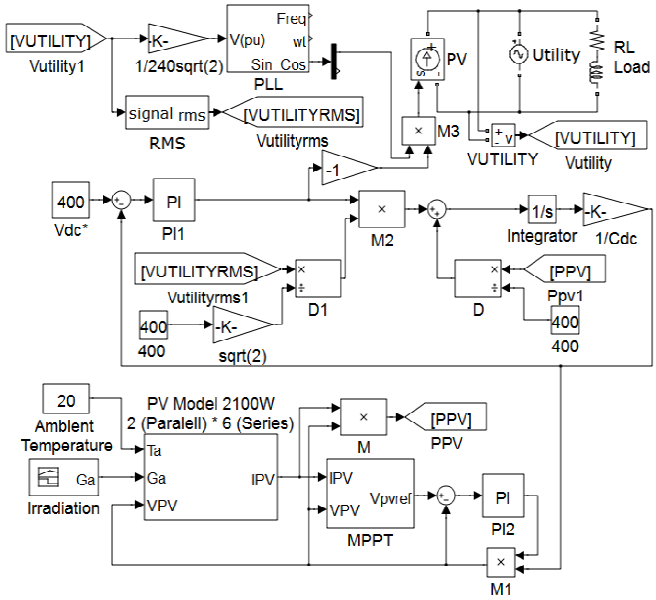

Fig. 7. Simplified current controlled source PV model [29]

2) Penetration Level

PV peak power has been used to calculate PV penetration, but in an uncontrolled environment PV peak power cannot be achieved because of ambient temperature. Therefore, in this study penetration level is defined as the ratio of total PV power under $1000W/m^2$ sun radiation and 35℃ ambient temperature to total system real power of all nominal loads, as well as for each spot load. For example, if the nominal real power of the load in Bus 675 phase-B is 120kW, then 40% PV penetration at this bus means 48kW PV power output under $1000W/m^2$ sun radiation and 35℃ ambient temperature conditions. The next section will discuss cloud effects of PV integration on voltage stability in residential areas.

III. Cloud Effects on Voltage Stability

Cloud effects can cause PV power fluctuations. Due to the fact that almost all PV systems only generate active power, traditionally power system frequency will be affected and vary with PV power. However, in distribution systems the R/X ratio of lines and cables is much larger than that in transmission systems, so real power variation can result in a comparable impact on grid voltage to reactive power. Moreover, in a small area (e.g. IEEE 13 bus) even for 40% PV penetration, losing all PV power only means approximately 1.5MW power deficit, which can be easily covered by the upstream transmission systems. Thus, in a distribution system, PV power fluctuation is closely related to voltage fluctuation rather than frequency.

Solar radiation can change very quickly. It has been reported that the quickest ramp rate can be $705W/m^2/s$, and it only takes a few seconds from a clear sky to heavy cloud cover [30, 31]. It was observed that a cloud traveled about $43feet/s$ in [31] and surely faster speeds may be expected in some areas under certain weather conditions, so a

geographically small area can be shaded by moving clouds within a short time.

On a hot summer day a local distribution network (e.g. the modified IEEE 13 bus) is heavily loaded and it mainly comprises room air conditioners. Meanwhile, PV panels can input a great amount of power to the grid under intensive sun irradiation with a high penetration level, therefore the voltage regulator does not detect a large load current and the tap changers are kept in relatively low positions. If clouds sweep over this network within a short time, PV power contribution will drop quickly. This will cause a large load increase for the upstream network and voltage drop will follow PV power decrease. A voltage regulator can observe a current increase; however the tap changer control scheme and mechanism stop it from responding immediately, so voltage drop cannot be compensated for until the tap changing delay exceeds a preset value. During this short period, voltage drop of some remote buses may have already developed to an unacceptable low level at which voltage stability cannot be maintained.

Next, the cloud effects on the IEEE 13 bus system with different PV penetration levels are investigated. PV systems are integrated into buses with spot loads in the network. The cloud transient is simulated by a decrease in solar irradiation from $1000W/m^2$ to $70W/m^2$ over a 20s period of time (from 10s to 30s, Fig. 8) and PV power generation declines with sunlight intensity. According to the tap changer control scheme the tap changing delay is chosen to be 30s for the first move and 5s for the following consecutive tap changes.

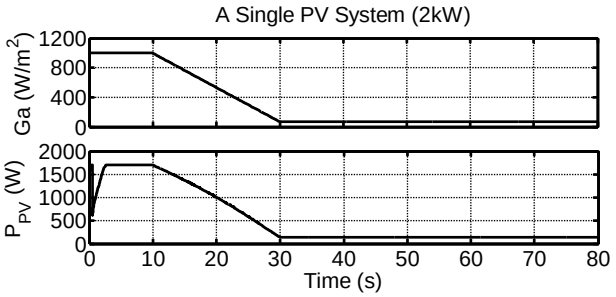

Fig. 8. PV power changes with sun irradiation

A. 0% Photovoltaic Penetration

Without any PV installation, the whole system becomes a traditional network. The simulation shows it can operate without voltage problems under a heavily loaded condition. The voltage profiles for all three phases are indicated in Fig. 9. Table IV shows allowable voltage ranges from the standard – ANSI C84.1 [32]. As discussed in Section II Part C, the normal voltage range of the 4.16kV service voltage should consider $\pm 10\%$ rather than $\pm 5\%$ when the voltage regulator range is taken into account. This may be against the voltage rating specification in the ANSI standard, but different applications do have different criteria. Therefore, in Fig. 9 all bus voltages are within an acceptable range.

Although Bus 675 and Bus 611 in phase-C have the lowest service voltages (Fig. 9), their utilization voltages (0.919 pu) still lie in Range A specified by the standard. Note that Bus 671 and Bus 684 also experienced low voltage comparable to Bus 675 and Bus 611, but they are located in upstream positions. Thus, if there are any voltage problems, Bus 675 and Bus 611 will show symptoms first. That is the reason why their voltage profiles have been examined in detail in Fig. 10.

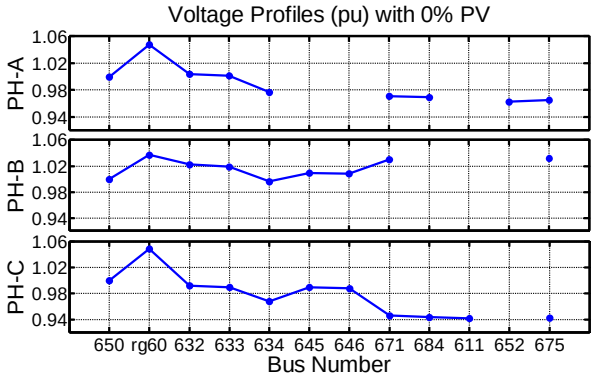

Fig. 9. Voltage profiles for all three phases without any PV systems

TABLE IV
VOLTAGE RATINGS – ANSI C84.1-2006 [32]

Ranges	Service Voltage (pu)	Utilization Voltage (pu)	Duration & Frequency	Corrective Measures
Range A	[0.950, 1.050]	[0.917, 1.042]	Indefinite	No Action Required
Range B	[0.917, 1.058]	[0.883, 1.058]	Limited & Infrequent*	Under-taken
Outside Range B	[0, 0.917] [1.058, ∞]	[0, 0.883] [1.058, ∞]	Limited & Infrequent*	Prompt Action

*: No specific frequency and time duration have been identified.

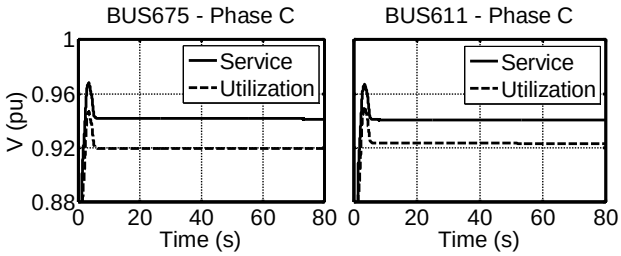

Fig. 10. Service and utilization voltages of Bus 675 and 611 phase-C (0% PV)

As can be seen from the simulation results, the distribution network was designed for the heavily loaded situation. Without any PV installation, the system will not suffer any disturbances due to variable generator integration, which is a great feature of a traditional network. However, power systems have entered an era of distributed generation and networks also need to perform well under power varying conditions, in which they were not designed to operate originally.

B. 10-30% Photovoltaic Penetration

The voltage profiles with 30% PV penetration are illustrated in Fig. 11. The solid lines show the bus voltages before cloud coverage and the dashed lines represent the voltages after the disturbance but before any reaction by the tap changer regulators. The voltage drop can indicate the bus voltage sensitivity to PV power decrease. As for 10% and 20% PV penetration, similar results were obtained with less voltage drop, so they are not presented in this paper.

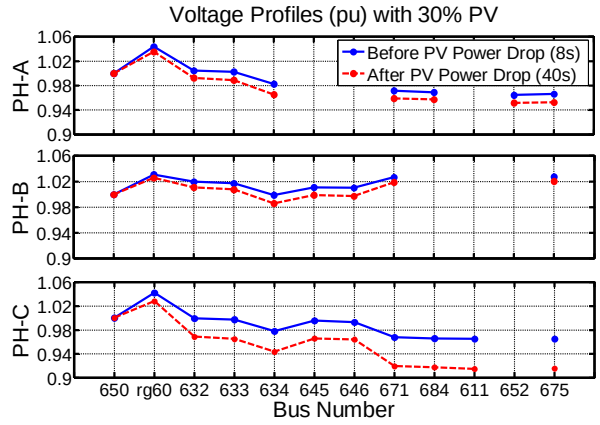

Fig. 11. Voltage profiles before and after cloud coverage

According to the results shown in Fig. 9 and Fig. 11, phase-C has the worst voltage profile and this is determined by the network configuration. Most of the loads in phase-B are placed in the upstream buses and its only load in remote Bus 675 is relatively small and over-compensated by a 200kVAr capacitor bank which results in reverse reactive power flow, so the voltage profiles in phase-B are much higher. Phase-A has large loads in the remote buses, but its total loading is almost a quarter less than that of phase-C, which results in less voltage drop. Therefore, although phase-A and phase-B are also heavily loaded (Table II), their voltage performances are much better than that of phase-C.

The voltages in Bus 675 and Bus 611 phase-C were most severely affected by cloud coverage. This is because they are both connected to large loads and situated in remote locations of the network. From the service voltage results, it is hard to identify which one is the weakest bus (about 0.05 pu voltage drop for both buses). However, theoretically Bus 675 with 396kW and 12kVAr loads tends to be more sensitive to voltage drop than Bus 611 with 170kW and -20kVAr loads, and the utilization voltage of Bus 675 is expected to have a lower value. This is confirmed by the results from the next part with 40% PV penetration (Fig. 12) as well as the results without PV (Fig. 10). Therefore, Bus 675 phase-C has the worst voltage profile and is the most sensitive bus to PV power drop and the following study will specifically focus on the performance of this bus.

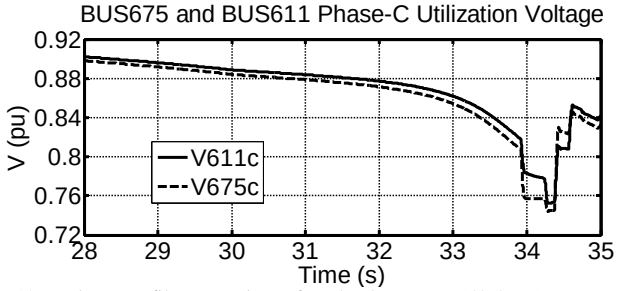

Fig. 12. Voltage profile comparison after cloud coverage (40% PV)

The voltage profiles in the worst bus (Bus 675) for different PV penetration levels due to the cloud transient effect are shown in Fig. 13. The major concern is the utilization voltage shortly after cloud coverage for 30% PV integration. It dropped to 0.891 pu for about 15s, however this is still within Range B and the corrective measure from the tap changer regulator was undertaken. The utilization voltage was driven back to Range A within 30s, which satisfied the ANSI standard.

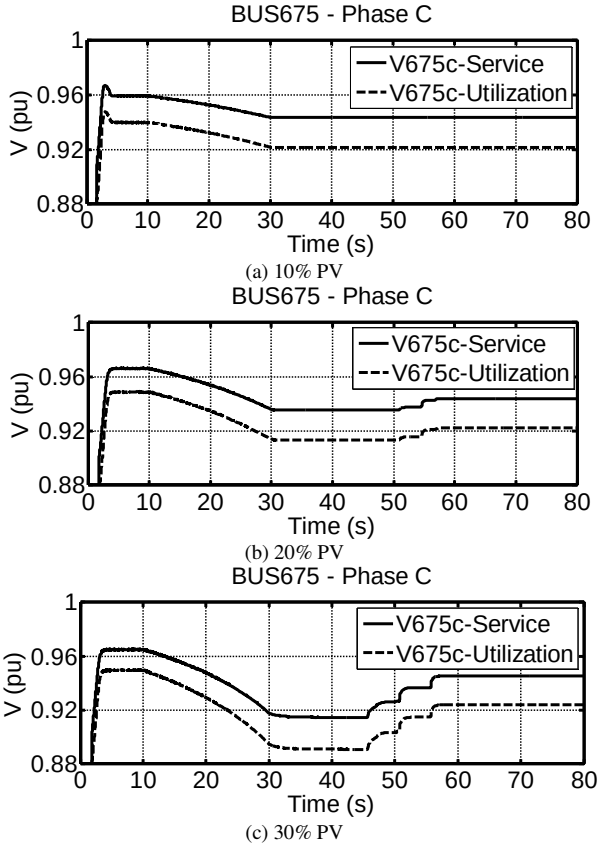

Fig. 13. Service and utilization voltages of Bus 675 phase-C with different PV penetration levels

C. 40% Photovoltaic Penetration

Fig. 14 shows the behavior of an induction motor load in Bus 675 phase-C. After the start up of the simulation, the system reached steady state at around 5s. From 10s clouds began to cover the local network area and the utilization voltage fell from the steady state voltage (0.957 pu). Because induction motors draw more current at a lower voltage, the voltage decrease continued after 30s until the induction motor stalled. When the motor speed slowed down to 40% of its synchronous speed the auxiliary circuit was reconnected consuming a great amount of power as motor starting. When its speed reached 80% the centrifugal switch opened, but the torque generated by the primary circuit was not enough to sustain the operation (Fig. 4 (b)), which resulted in a stalling motor again. During the induction motor stalling the utilization voltage went as low as 0.74 pu (Fig. 15). Such stalling cycle repeated a few times until the thermal protection device disconnected the induction motor from the grid. Soon after, the bus voltage recovered. As shown in Table V, tap changers did react when the load current increased, however they could not support the voltage fast enough to prevent instability.

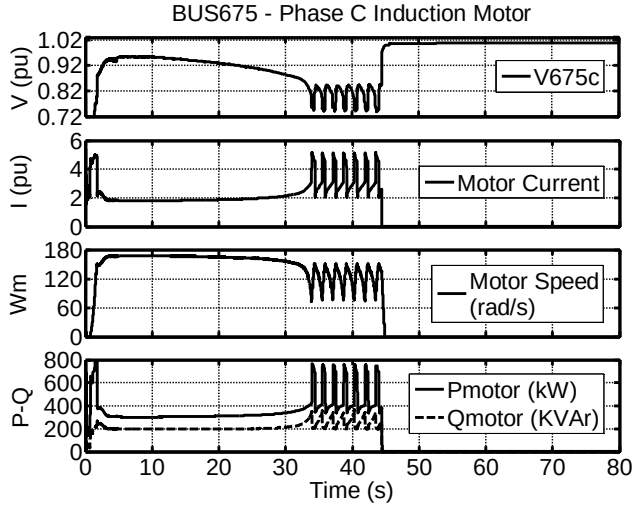

Fig. 14. Induction motor load in Bus 675 phase-C

Depending on the control and protection schemes chosen, the system characteristics may vary as follows.

(1) Without any additional information on induction motor control and protection, only the most common protection devices – thermal relays are equipped for all induction motors. If under-voltage relays are implemented, the motor may be disconnected from the grid before it stalls.

(2) For different motor control and starting strategies, the cut-in/cut-out stalling effect may not occur. For example, if the torque generated by the auxiliary circuit is smaller than the load torque under low voltage, or the compressor pressure is much greater than the torque available, a motor will remain stalled until disconnection by its thermal protection.

(3) The motors at the remote buses had stalled for approximately 10s and during this period the motor current almost tripled. This made the total power in phase-C seen from the substation (Fig. 16 and Table VI) much greater than the transformer rating. If the protection acts quicker in the substation, phase-C will be separated shortly after stalling. Then the cut-in/cut-out stalling effect may end earlier.

However, all these possible variations cannot change the fact that when a voltage stability problem is caused by cloud coverage within a short period in the modified IEEE 13 bus system with 40% PV penetration, at least one branch or some appliances must be removed from the power grid of phase-C to restore bus voltages.

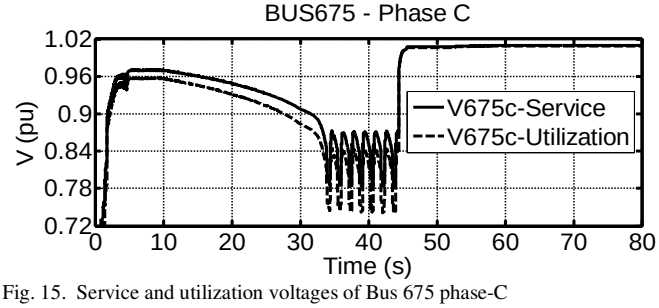

Fig. 15. Service and utilization voltages of Bus 675 phase-C

TABLE V
TAP CHANGER POSITIONS OF THE IEEE 13 BUS SYSTEMS

Time	Tap Position		
	Phase-A	Phase-B	Phase-C
8s	14	9	12
80s	16	11	13

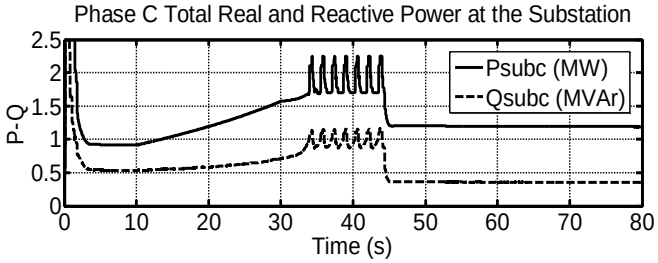

Fig. 16. Total power in phase-C of the substation

TABLE VI
PHASE-C REAL AND REACTIVE POWER AT SUBSTATION

	Normal Operation	During Stalling
P_{subC} (MW)	0.914	1.692 – 2.253
Q_{subC} (MVAr)	0.537	0.867 – 1.164

IV. VOLTAGE STABILITY USING STATIC LOAD MODELS

For 40% PV penetration the voltage stability problem was investigated by implementing detailed dynamic loads. If the static load models are used, voltage instability cannot be identified.

The simulation was conducted under the same PV disturbance, PV penetration and nominal load power as in Section III Part C. All the detailed loads were replaced by the static loads specified in [20] – ZIP loads.

As illustrated in Fig. 17, before the decrease of PV power the steady state results from time domain simulation were almost the same for both networks with static and detailed dynamic loads at 8s. Fig. 15 showed an unstable voltage profile of Bus 675 phase-C and its utilization voltage was as low as 0.74 pu. The induction motor stalled and consumed several times the rated power. However, the simulation with static loads indicated that the lowest utilization voltage was 0.9 pu, which lies in Range B of Table IV and within about 30s the utilization voltage would be increased back to Range A by the voltage regulator. Thus, no voltage stability problem was observed when the static load models were used. The reasons for this can be explained as follows:

(1) High PV Penetration: With more PV power integrated into the system (40%), voltage regulators at the beginning of the feeder will observe less equivalent loads P_{Load}-P_{PV} (smaller line currents) than those at lower PV penetration levels. Therefore, tap changers will operate at lower positions. When there is a sudden loss in PV power more equivalent loads will be seen by the voltage regulator compared with lower penetrations levels, which results in more voltage drop along the line before the voltage regulator can operate. Thus, more voltage drops with lower tap

positions cause lower voltages towards the end of the feeder which exacerbates voltage stability.

(2) Load Models: When the network loses PV power support, generally bus voltages will decrease.
   (a) For steady load models the loading power will be reduced for constant impedance loads and constant current loads and no change will occur for constant power loads (majority). In summary, the total power will decrease when losing PV power. To some extent this alleviates the voltage drop situation.
   (b) For dynamic load models the response for resistive loads is the same as those in steady models. Thermostatic loads will slowly recover their power consumption. Moreover, induction motor loads (room air-conditioners) will increase in real power as the bus voltages decrease (shown in Fig.2). Their reactive power will first decline. With further voltage drop, the reactive power consumption will increase, which makes voltage drop worse and causes voltage stability issues.

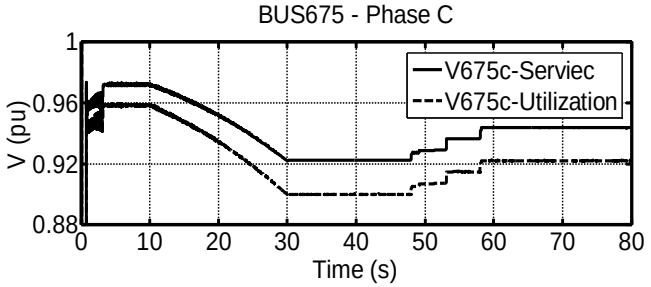

Fig. 17. Service and utilization voltages of Bus 675 phase-C using static load models (40% PV)

V. Potential Solutions

There are a number of potential methods to solve voltage stability problems related to PV power fluctuations. First, energy storage can be a potential solution to the problem. This approach should be effective since the voltage instability addressed previously is caused by real power drop from PV. However, this is going to be an expensive solution. Currently, a Zinc-Bromine (ZnBr) flow battery unit with a capacity of 5kVA-20kWh costs around 20,000 Australian dollars (AU$) [33]. Installing distribution static compensators (DSTATCOM) can also mitigate the voltage problem. The reported price is roughly 50-55 US$/kVar for small STATCOM units [34], so this may be a cheaper choice compared to storage devices.

Another solution is to re-conductoring the feeder with larger size conductors, which can reduce line voltage drops. This will definitely provide a strong foundation for the distribution network. However, considering the number of feeders that needs to be upgraded in distribution networks, re-conductoring may not be a cheap option either. A local electricity utility estimates that replacing wires for a single phase system could cost around 25,000 AU$/km [33]. Last but not least, network re-configuration (rearranging the load and PV power between phases) may be a practical scheme that can be used to improve voltage profiles. This method can utilize the potential of the network itself and may not cost much to realize. However, more research and planning work is needed before re-configuration becomes possible. Among all these possible techniques, only energy storage solution and PV reactive power support are analyzed below. Other possibilities will be investigated in our future research.

A. Battery Storage

The storage solution was investigated with storage units consisting of 20% of total power installed at Bus 650 behind the substation transformer (at 4.16kV side) to compensate for PV power variations. This implies that the PV penetration level is reduced from 40% to 20% effectively and according to the study in Section III Part B, a power swing of 20% PV will not result in a voltage stability problem. However, cloud induced PV power fluctuations can still cause voltage instability as shown in Fig. 18. This is due to the position of the storage. When all storage units are arranged at the beginning of the feeder the current flowing in the line will not decrease much as the battery current needs to feed loads through the line. Therefore, this configuration cannot properly reduce voltage drop along the line.

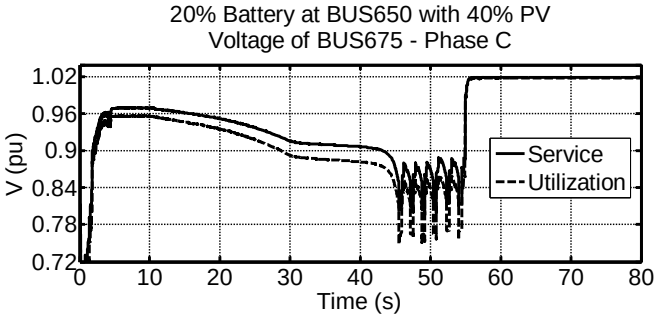

Fig. 18. Bus 675 phase-C voltage with 20% storage at Bus 650 behind the substation transformer (40% PV)

If all storage units are located at Bus 632 (2000ft downstream from Bus 650) the voltage drop will be reduced. Therefore, voltage instability can be avoided (Fig. 19).

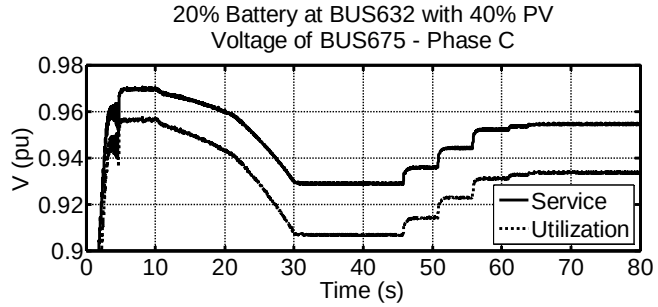

Fig. 19. Bus 675 phase-C voltage with 20% storage at Bus 632 (40% PV)

In summary, storage devices can be effective for the presented issue, but they should be located in a downstream position to reduce line voltage drop. Otherwise, the storage can

only delay voltage instability for a short period and will not solve the problem.

B. PV Reactive Power Support

Another attractive approach of solving the voltage problem is reactive power support through PV inverters. Normally, PV produces less real power than the rated capacity of its inverter, which leaves space for reactive power generation. Especially when grid voltage drops are caused by loss of PV real power, there will be more room for reactive power support. Over the years, many reactive power generation schemes have been proposed [9-11, 16, 35-36]. Based on these methods, a PV reactive power control strategy is developed in this section (Fig. 20), which takes the following considerations into account.

(1) Real power generation has the priority. Since reactive power generation does not provide any financial benefits in return and instead put more stress to inverters which shortens their lifetime, this control strategy gives generation priority to real power in order to maximize the owners' profit. That is the reason why the real current component ($I^*_{ref\_Re}$) has the full current limit of the inverter and the react current component ($I^*_{ref\_Im}$) has dynamic limits depending on real power generation. When there are not any concerns on voltage magnitude at the point of common coupling (PCC), no reactive power is produced in order to reduce the burden of PV inverters under normal operational conditions ($\alpha \approx 0$ for $0.95 \le V_{PCC\_rms} \le 1.02$ Fig. 21).

(2) The reactive capacity is gradually released based on grid voltage levels at the PCC. This reduces oscillations at the boundaries of the reactive power control coefficient α.

(3) The parameters are selected according to the standards and common practices. For example, the values of coefficient α are chosen with respect to different voltage levels at the PCC in Fig. 21 based on the voltage rating standard [32] with reasonable margins. The simulated PV real power generation at 35℃ and $1000W/m^2$ is assumed to account for 80% of the rated inverter capacity. These values may be adjusted if this control strategy is implemented for different applications.

Fig. 22 shows the simulation results when the developed control strategy is implemented in the PV systems. Compared to the unity power factor scenario with an unstable voltage at Bus 675 phase-C (Fig. 15), the voltage profile with PV reactive power support indicates a much better performance. Before 10s, the voltage was greater than 0.95 pu threshold, so the coefficient α was very close to zero. Little reactive power was generated. Then PV real power started to decrease due to cloud coverage. When the grid voltage declined below 0.95 pu, reactive power support became effective, which reduced the voltage drop rate from around 15s. From approximately 46s, the auto tap changer began its voltage regulation process and reactive power generation was decreased with the increase in the grid voltage.

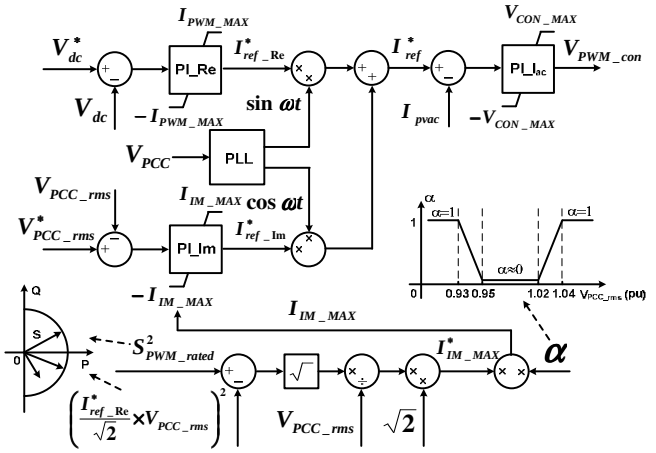

Fig. 20 PV reactive power control strategy

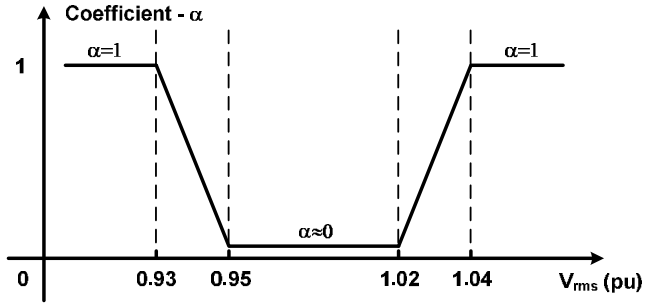

Fig. 21 Coefficient α for reactive current limits

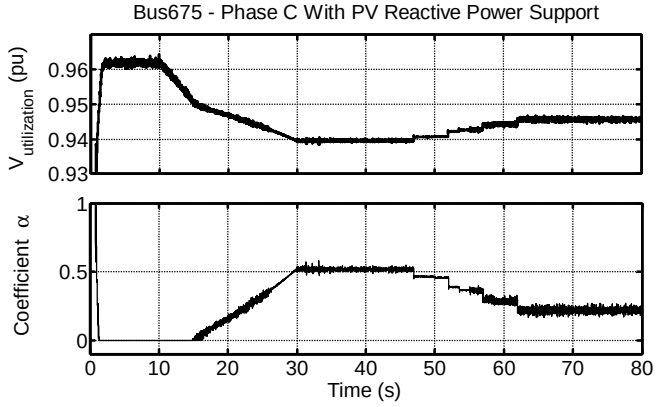

Fig. 22 Voltage performance of Bus 675 phase-C and the coefficient control signal α with PV reactive power support

Although reactive power generation for voltage regulation is against the current standards [12-13, 37], the simulation results demonstrate the benefit and effectiveness of PV inverter reactive power support if it is allowed in the near future.

VI. Simulation Results Summary

The simulation results are summarized in Table VII and the following observations can be made:

(1) The traditional distribution network operates under a loading level close to the rating without voltage problems.

(2) The network still can maintain voltage stability with 10-30% PV penetration levels when the local area is covered by fast moving clouds. The worst voltage (0.891 pu) is still within the allowed range (Range B).
(3) Voltage stability of the system cannot be maintained with 40% PV penetration under the same radiation disturbance. The induction motors in Bus 675 phase-C is stalled under the low grid voltage before the voltage support action by the voltage regulator. Eventually, the induction motor loads are disconnected by their thermal protection units and the grid voltage is recovered to normal.
(4) The same problem was not observed when static load models were applied. The lowest recorded voltage was 0.9 pu, which was in Range B and the voltage was brought back to 0.922 pu (Range A) in a short time.
(5) With 20% storage units, which are controlled to smooth PV power fluctuations, voltage stability can be maintained. However, storage locations should be carefully chosen for maintaining voltage stability.
(6) The PV inverter reactive power control scheme was extremely effective for fast voltage support. All voltage magnitudes were regulated within the limits defined in the standard (Table IV).

TABLE VII
BUS 675 VOLTAGE PROFILES WITH DIFFERENT PV PENETRATION LEVELS AND LOAD MODELS

Load	Penetration	Voltage Status	V675 phase-C (pu) Service and Utilization (in bracket)		
			t=8s	t=40s	t=80s
Dynamic	0%	Stable	0.941 (0.919)	0.941 (0.919)	0.941 (0.919)
Dynamic	10%	Stable	0.960 (0.940)	0.943 (0.922)	0.943 (0.922)
Dynamic	20%	Stable	0.966 (0.949)	0.936 (0.914)	0.944 (0.922)
Dynamic	30%	Stable	0.965 (0.949)	0.915 (0.891)	0.945 (0.924)
Dynamic	40%	Unstable	0.970 (0.957)	0.783 (0.739) - 0.872 (0.845)	1.010 (1.009)
Static	40%	Stable	0.972 (0.958)	0.922 (0.900)	0.944 (0.922)
Dynamic	40% PV + 20% Storage (Bus650)	Unstable	0.970 (0.957)	0.809 (0.762) - 0.886 (0.857)	1.009 (1.004)
Dynamic	40% PV + 20% Storage (Bus632)	Stable	0.970 (0.957)	0.929 (0.907)	0.955 (0.934)
Dynamic	40% PV + PV Reactive Support	Stable	0.973 (0.961)	0.955 (0.940)	0.964 (0.946)

VII. DISCUSSIONS: IMPORTANT OBSERVATIONS

At each bus, PV penetration has been proportionate to its load. For example, for 10% PV penetration, PV installation at each bus is 0.1 times the load of that bus. The IEEE 13 bus system is assumed to be heavily loaded and located in a geographically small area. However, some key observations can be made with the following three questions:

(i) What will happen if PVs are distributed differently rather than proportionally distributed?
(ii) What will happen if geographically the network is situated in a relatively large area?
(iii) What will happen if the IEEE 13 bus has a different loading level?

The authors have recently observed that PV power variation in each phase have different contributions to voltage changes of other phases because of the mutual coupling of the unbalanced line configuration. For example, in the backbone lines (from Bus 650 to Bus 671) of the IEEE 13 bus system, phase-C voltage decreases with a PV power drop to phase-A and phase-C, but it increases with a PV power drop to phase-B.

If PV units are not allocated as has been assumed in this paper – being proportionate to the load of each bus, the results may be different based on the observations mentioned above. For example, if more PV power is installed in phase-B and less PV has been integrated into phase-A and phase-C (compared with the proportional installation), phase-C voltage variations due to PV power changes will be much smaller than that of a proportionally distributed situation. Thus, voltage instability presented in this paper may be avoided. On the contrary, with less PV power in phase-B and more in phase-A and phase-C, the voltage drop of phase-C will be greater than that of the proportional case, so voltage problems can still occur.

If phase-A and phase-C branches are mainly located in close proximity to each other in a geographically small area which may be covered by clouds within a short time the problem presented in the paper is still likely to occur based on the observations even though the whole network is in a relatively large area.

If the loading level is low (e.g. winter time), voltage drop may not be serious enough to result in voltage instability when PV power is reduced within a short period of time. The voltage problem presented may happen if the tap positions are further lowered by a higher PV penetration level.

These discussions are beyond the scope of this paper. The basis of the unbalanced analysis can be found in the authors' paper – [38].

VIII. CONCLUSIONS

This paper investigated the distribution network voltage stability problem in geographically small residential areas with high PV penetration levels. The small-scale PV systems are based on the current standards and industrial practices without reactive power generation. The simulation results showed voltage instability occurred in 40% PV power integration for a heavily loaded network when the cloud induced voltage fluctuations developed faster than the reaction of the voltage regulator. Because of the uniqueness of distribution systems, voltage stability caused by high PV integration may become an important issue and it needs to be thoroughly examined.

Distribution networks were designed for heavy loading conditions without any PV integration, but they still can

operate well with low PV penetration levels. Cloud effects on voltage stability became a serious concern for the studied system when 40% power was contributed from PV systems in a geographically small area. This issue may not be identified properly when the loads were modeled as static loads. Therefore, detailed dynamic load models are recommended for PV integration studies. However, this 40% limit may vary for different distribution networks.

One energy storage solution has been discussed in this paper. Simulation results showed that although the equivalent PV penetration was brought down by the storage units to a seemly safe level – 20%, the presented voltage stability problem may still occur if the storage source is installed at the beginning of the feeder. The problem can be solved by selecting the storage position properly in a downstream bus to reduce voltage drops along the distribution line.

A PV inverter reactive power support scheme has been developed to solve the voltage stability problem instead of installing extra compensation devices. The simulation results showed the effectiveness of this method and proved it is beneficial for the distribution network.

This study demonstrates a potential voltage stability problem caused by fast PV power fluctuations if the current standards and industrial practices for small-scale PV systems (no reactive power generation for voltage regulation) are still kept the same in a high PV penetration era. However, if reactive compensation of PV inverters is allowed when grid voltage at the PCC becomes too low or too high the voltage problem can effectively be solved.

APPENDIX

The load combination at each node is shown in Table VIII.

TABLE VIII
LOAD COMBINATIONS AT EACH NODE AFTER LOAD MODIFICATION

Bus	Phase	Bus Loads		Motor Power		Resistive Power	Percentage (*/Ptotal)	
		P (kW)	Q (kVAr)	P (kW)	Q (kVAr)	P (kW)	Pmotor %	Presist %
Bus634	Ph-A	160	110	152	108	8	95%	5 %
	Ph-B	181	90	124	88	57	69%	31%
	Ph-C	168	90	124	88	44	74%	26%
Bus645	Ph-B	251	125	172	123	79	69%	31%
Bus646	Ph-B	230	132	182	129	48	79%	21%
Bus652	Ph-A	128	86	119	84	9	93%	7%
Bus671	Ph-ABC	385	220	303	216	82	79%	21%
Bus675	Ph-A	485	190	262	186	223	54%	46%
	Ph-B	120	60	83	59	37	69%	31%
	Ph-C	396	212	292	208	104	74%	26%
Bus692	Ph-C	282	151	208	148	74	74%	26%
Bus611	Ph-C	170	80	110	78	60	65%	35%
Total	Ph-A	1175	616	849	604	326	72%	28%
	Ph-B	1233	665	917	652	316	74%	26%
	Ph-C	1518	821	1132	805	386	75%	25%
Total		3926	2102	2898	2060	1028	74%	26%

In the table, the load combination at some nodes is not close to 75% motor loads with 25% resistive loads. The reason for this is the original Real/Reactive (P/Q) load ratios of the nodes in the IEEE 13 bus system. If a node has a large P/Q ratio, it probably indicates more resistive loads are connected to this node. For example, Bus675 phase-A is a node of this kind, including 54% motor loads and 46% resistive loads. While, Bus652 phase-A has a small P/Q ratio, and it contains 93% motor loads. However, for each phase or the whole feeder, the 25%-75% load combination should be held roughly. This is highlighted in the table with the underlined numbers. According to all of these arrangements, a condensed form of information was given in the paper as Table III.

REFERENCES

[1] E. Liu and J. Bebic, "Distribution system voltage performance analysis for high-penetration photovoltaics," *NREL/SR-581-42298*, Tech. Rep., 2008. [Online]. Available: http://www1.eere.energy.gov/solar/pdfs/42298.pdf.

[2] S. Achilles, S. Schramm, and J. Bebic, "Transmission system performance analysis for high-penetration photovoltaics", *NREL/SR-581-42300*, Tech. Rep., 2008. [Online]. Available: http://www1.eere.energy.gov/sol-ar/pdfs/42300.pdf.

[3] C. Whitaker, J. Newmiller, M. Ropp, and B. Norris, "Distributed photovoltaic systems design and technology requirements", *SAND2008-0946 P, Sandia National Laboratories,* Tech. Rep., 2008. [Online] Available:http://www1.eere.energy.gov/solar/pdfs/distributed_pv_system_design.pdf.

[4] M. McGranaghan, T. Ortmeyer, D. Crudele, T. Key, J. Smith, and P. Baker, "Advanced grid planning and operations", *NREL/SR-581-42294/SAND2008-0944 P*, Tech. Rep., 2008. [Online] Available: http://www1.eere.energy.gov/solar/pdfs/advanced_grid_planning_operations.pdf.

[5] S. Conti, A. Greco, N. Messina, and S. Raiti, "Local voltage regulation in LV distribution networks with PV distributed generation", *International Symposium on Power Electronics, Electrical Drives, Automation and Motion, 2006. SPEEDAM 200,* pp. 519-524, 2006.

[6] E. Demirok, D. Sera, R. Teodorescu, P. Rodriguez, and U. Borup, "Clustered PV inverters in LV networks: An overview of impacts and comparison of voltage control strategies", *Electrical Power & Energy Conference (EPEC), 2009 IEEE* pp. 1-6, 2009.

[7] D. T. Ton, C. J. Hanley, G. H. Peek, and J. D. Boyes, "Solar energy grid integration systems – energy storage (SEGIS-ES)", *SAND2008-4247, Sandia National Laboratories*, Tech. Rep., 2008. [Online]. Available: http://www1.eere.energy.gov/solar/pdfs/segis-es_concept_paper.pdf.

[8] N. Kakimoto, H. Satoh, S. Takayama, and K. Nakamura, "Ramp-rate control of photovoltaic generator with electric double-layer capacitor", *IEEE Trans. Energy Conversion,* vol. 24, pp. 465-473, 2009.

[9] P.M.S. Carvalho, P.F. Correia, and L.A.F. Ferreira, "Distributed Reactive Power Generation Control for Voltage Rise Mitigation in Distribution Networks", *IEEE Trans. Power Systems*, vol. 23, pp. 766-772, 2008.

[10] R.A. Mastromauro, M. Liserre, T. Kerekes, and A. Dell'Aquila, "A single-phase voltage-controlled grid-connected photovoltaic system with power quality conditioner functionality", *IEEE Trans. Industrial Electronics,* vol. 56, pp. 4436-4444, 2009.

[11] J.C. Vasquez, R.A. Mastromauro, J.M. Guerrero, and M. Liserre, "Voltage support provided by a droop-controlled multifunctional inverter", *IEEE Trans. Industrial Electronics,* vol. 56, pp. 4510-4519, 2009.

[12] "IEEE Recommended Practice for Utility Interface of Photovoltaic (PV) Systems," *IEEE Std 929-2000,* 2000.

[13] "IEEE Standard for Interconnecting Distributed Resources with Electric Power Systems," *IEEE Std 1547-2003,* pp. 0_1-16, 2003.

[14] T. Senjyu, Y. Miyazato, A. Yona, N. Urasaki, and T. Funabashi, "Optimal Distribution Voltage Control and Coordination With Distributed Generation", *IEEE Trans. Power Delivery*, vol. 23, pp. 1236-1242, 2008.

[15] M. Kim, R. Hara, and H. Kita, "Design of the Optimal ULTC Parameters in Distribution System With Distributed Generations", *IEEE Trans. Power Systems*, vol. 24, pp. 297-305, 2009.

[16] P. N. Vovos, A. E. Kiprakis, A. R. Wallace, and G. P. Harrison, "Centralized and Distributed Voltage Control: Impact on Distributed

Generation Penetration", *IEEE Trans. Power Systems*, vol. 22, pp. 476-483, 2007.
[17] T. Yun Tiam and D. S. Kirschen, "Impact on the power system of a large penetration of photovoltaic generation", *Power Engineering Society General Meeting, 2007. IEEE,* pp. 1-8, 2007.
[18] R. Tonkoski and L.A.C. Lopes, "Voltage Regulation in Radial Distribution Feeders with High Penetration of Photovoltaic", *Energy 2030 Conference, 2008. ENERGY 2008. IEEE.*, pp. 1-7, 2008.
[19] PSCAD, http://pscad.com.
[20] "IEEE 13 Node Test Feeder", IEEE Power Engineering Society, 2009. [Online]. Available: http://ewh.ieee.org/soc/pes/dsacom/testfeeders/index.html.
[21] K. Morison, H. Hamadani, and L. Wang, "Load Modeling for Voltage Stability Studies", *Power Systems Conference and Exposition, PSCE '06, IEEE PES*, pp. 564-568, 2006.
[22] C. W. Taylor, *Power System Voltage Stability*, New York : McGraw Hill, 1994, pp. 67-107.
[23] P. Kundur, *Power System Stability and Control*, New York : McGraw Hill, 1994, pp. 271-314, 959-1024.
[24] A.E. Fitzgerald, C. Kingsley, S. D. Umans, *Electric Machinery (6th Edition)*, Boston : McGraw Hill, 2003, pp. 452-492.
[25] P. C. Krause, *Analysis of electric machinery and drive systems (2nd Edition)*, New York : IEEE Press, 2002, pp. 361-393.
[26] "SYNCROSNAP® Centrifugal Switches for Single-Phase Electric Motors", *Product Information*, *TORQ Corporation,* [Online]. Available: http://www.torq.com/pdffiles/centrifugalswitches.pdf.
[27] W. H. Kersting, *Distribution System Modeling and Analysis*, Boca Raton : CRC Press, 2007.
[28] T. V. Cutsem and C. Vournas, *Voltage Stability of Electric Power Systems*, Boston, Mass. [u.a.] : Kluwer Acad. Publ., 1998, pp. 93-133.
[29] R. Yan, T. K. Saha, "Development of Simplified Models for a Single Phase Grid Connected Photovoltaic System", Proceeding of *the Australasian Universities Power Engineering Conference 2010, IEEE. (AUPEC)* Christchurch, New Zealand from 5th-8th December.
[30] T. Tomson, "Fast dynamic processes of solar radiation", *Solar Energy*, vol. 84, pp. 318-323, 2010.
[31] E. C. Kern Jr., E. M. Gulachenski, and G. A. Kern, "Cloud effects on distributed photovoltaic generation: slow transients at the Gardner, Massachusetts photovoltaic experiment", *IEEE Trans. Energy Conversion*, vol. 4, pp. 184-190, 1989.
[32] "American National Standard for Electric Power Systems and Equipment – Voltage Ratings (60 Hertz)", *National Electrical Manufacturers Association (NEMA), American National Standards Institute, Inc., ANSI C84.1-2006*, 2006.
[33] M. Zillmann, R. Yan and T. K. Saha, "Regulation of Distribution Network Voltage Using Dispersed Battery Storage Systems: A Case Study of a Rural Network", Proceeding of *the IEEE PES General Meeting 2011* in Detroit, Michigan, USA, during July 24-28, 2011.
[34] M. Molinas, Suul Jon Are, T. Undeland, "Low Voltage Ride Through of Wind Farms With Cage Generators: STATCOM Versus SVC", *IEEE Trans. Power Electronics*, vol. 23, pp. 1104-1117, 2008.
[35] G.M.S. Azevedo, P. Rodriguez, M.C. Cavalcanti, G. Vazquez, and F.A.S. Neves, "New control strategy to allow the photovoltaic systems operation under grid faults" *Power Electronics Conference, 2009. COBEP '09. Brazilian*, 2009, pp. 196-201.
[36] K. Turitsyn, P. Sulc, S. Backhaus, and M. Chertkov, "Distributed control of reactive power flow in a radial distribution circuit with high photovoltaic penetration" *The IEEE PES General Meeting 2010* pp. 1-6.
[37] "Grid connection of energy systems via inverters," *Australian Standard, AS4777-2005,* 2005.
[38] R. Yan, T. K. Saha, "Investigation of Voltage Variations in Unbalanced Distribution Systems due to High Photovoltaic Penetrations", Proceeding of *the IEEE PES General Meeting 2011* in Detroit, Michigan, USA, during July 24-28, 2011.

BIOGRAPHIES

Ruifeng Yan (S'2009) received the B. Eng. (Hons.) degree in Automation from University of Science and Technology, Beijing, China, in 2004 and the M. Eng degree in Electrical Engineering from the Australian National University, Canberra, Australia, in 2007. He is currently pursuing Ph.D. degree in power and energy systems at the University of Queensland, Brisbane, Australia.

Tapan K. Saha (SM'97) was born in Bangladesh and immigrated to Australia in 1989. Currently, he is Professor of Electrical Engineering in the School of Information Technology and Electrical Engineering, University of Queensland, Brisbane, Australia. Before joining the University of Queensland, he taught at the Bangladesh University of Engineering and Technology, Dhaka, for three-and half years and then at James Cook University, Townsville, Australia, for two and half years. His research interests include power systems, power quality, and condition monitoring of electrical plants. Dr. Saha is a Fellow of the Institution of Engineers, Australia.